



Published in final edited form as:

Urol Oncol. 2016 July ; 34(7): 311–319. doi:10.1016/j.urolonc.2016.03.001.

Prostate cancer risk stratification with magnetic resonance imaging

Ely R. Felker, M.D.^a, Daniel J. Margolis, M.D.^a, Nima Nassiri, M.D.^b, and Leonard S. Marks, M.D.^{b,*}

^aDepartment of Radiology, Ronald Reagan-UCLA Medical Center, Los Angeles, CA

^bDepartment of Urology, David Geffen School of Medicine, Los Angeles, CA

Abstract

In recent years, multiparametric magnetic resonance imaging (mpMRI) has shown promise for prostate cancer (PCa) risk stratification. mpMRI, often followed by targeted biopsy, can be used to confirm low-grade disease before enrollment in active surveillance. In patients with intermediate or high-risk PCa, mpMRI can be used to inform surgical management. mpMRI has sensitivity of 44% to 87% for detection of clinically significant PCa and negative predictive value of 63% to 98% for exclusion of significant disease. In addition to tumor identification, mpMRI has also been shown to contribute significant incremental value to currently used clinical nomograms for predicting extraprostatic extension. In combination with conventional clinical criteria, accuracy of mpMRI for prediction of extraprostatic extension ranges from 92% to 94%, significantly higher than that achieved with clinical criteria alone. Supplemental sequences, such as diffusion-weighted imaging and dynamic contrast-enhanced imaging, allow quantitative evaluation of cancer-suspicious regions. Apparent diffusion coefficient appears to be an independent predictor of PCa aggressiveness. Addition of apparent diffusion coefficient to Epstein criteria may improve sensitivity for detection of significant PCa by as much as 16%. Limitations of mpMRI include variability in reporting, underestimation of PCa volume and failure to detect clinically significant disease in a small but significant number of cases.

Keywords

MRI; Prostate cancer; Risk stratification

Introduction

Multiparametric magnetic resonance imaging (mpMRI) is an increasingly useful tool for prostate cancer (PCa) detection and risk assessment, allowing noninvasive assessment of the entire organ from both an anatomic and a functional perspective. A recent meta-analysis demonstrated sensitivity ranging from 44% to 87% for the detection of clinically significant PCa and negative predictive value (NPV) ranging from 63% to 98% for exclusion of clinically significant PCa [1]. In addition to PCa detection, there is an expanding body of

*Corresponding author. Tel.: +310-710-3873; fax: 131-0794-3060. lmarks@mednet.ucla.edu, lsmarks@ucla.edu (L.S. Marks).

evidence to support the use of mpMRI for PCa risk stratification [2–4]. Among men with low-risk disease, mpMRI can assess both initial and continuing suitability for active surveillance (AS); among men with intermediate or high-risk disease, mpMRI can add useful information about the likelihood of extraprostatic extension (EPE) and whether nerve-sparing treatments are possible.

History of prostate MRI

The use of MRI in PCa was first described in 1983 [5]. Prostate MRI was initially used mainly as a locoregional staging tool in selected patients with known PCa. Prostate MRI in this era had very limited ability to distinguish aggressive PCa from benign pathologic tissue.

Technological advancements, such as higher field-strength magnets, endorectal coils, and adoption of supplementary sequences, coupled with increasing investigator experience and research led to the development of mpMRI. The ability to combine anatomic and functional assessment of the prostate has expanded the scope of use dramatically. Prostate mpMRI is now used for tumor detection, tumor characterization, biopsy planning, and surveillance, in addition to locoregional staging.

mp Prostate MRI

Contemporary prostate mpMRI involves anatomic and functional sequences. These most commonly include T1-weighted and T2-weighted sequences combined with diffusion-weighted imaging (DWI) and dynamic contrast-enhanced (DCE) imaging. Magnetic resonance spectroscopy is occasionally used but is limited by interreader variability and technical issues.

T2-weighted imaging

T2-weighted imaging (T2WI) remains the standard for anatomic assessment of the prostate because of its superior soft tissue resolution. In addition to tumor localization, T2WI can be used to depict the prostate capsule, neurovascular bundles, anterior fibromuscular stroma, and seminal vesicles. For this reason, T2WI is the primary sequence used for locoregional staging. EPE can be demonstrated as direct extension of tumor into the periprostatic fat, capsular bulging or irregularity, or decreased signal in the seminal vesicles. T2WI is also of utmost importance for assessment of the transition zone, where changes of benign prostatic hyperplasia (BPH) may be difficult to distinguish from PCa. Nonencapsulation, homogeneously low-signal intensity, and the characteristic “erased charcoal” appearance are useful features for identification of transition zone tumors [6,7]. EPE or seminal vesicle invasion (SVI) may also be noted.

Diffusion-weighted imaging

DWI evaluates the motion of water molecules in the body. In an unrestricted environment, water movement is random, so-called Brownian motion. Movement of water molecules in biologic tissues is restricted because of interactions with cell membranes and intracellular organelles. The degree of restriction to water diffusion is inversely related to tissue cellularity and the integrity of cell membranes [8]. The magnitude of diffusion can be measured using the apparent diffusion coefficient (ADC), which represents the slope of the

line calculated by plotting the logarithm of relative signal intensity (y -axis) against b -values (x -axis). The b -value refers to the strength of the diffusion-sensitizing gradient. In clinical practice, 2 or more b -values are acquired with one typically greater than 1000 s/mm². DWI was first widely applied in neuroimaging for detection of acute stroke [9]. Its use in oncology has since grown markedly, because rapidly growing tumors with densely cellular tissues have more water restriction than normal tissue. PCa demonstrates high signal relative to normal prostate on high b -value DWI and low-signal intensity on the ADC map. A recently performed meta-analysis evaluated the use of DWI for PCa detection. Pooled sensitivity and specificity across 21 included studies were 0.62 and 0.90, respectively, with an area under the curve (AUC) of 0.8991 [10]. In addition to detection, tumor ADC has been shown to be a useful marker in initial selection of men for AS. In a 9-year follow-up study, Henderson et al. [11], recently showed that ADC below the median was associated with shorter time to adverse histology and shorter time to radical treatment.

DCE imaging

DCE-MRI is performed using a fast T1W gradient echo sequence repeated at short intervals before, during, and after the intravenous injection of low molecular weight gadolinium chelate. PCa prognosis is inversely related to the number of abnormal blood vessels in the tissue [12,13]. PCa microvessel density has also been shown to be an independent predictor of pathologic stage [14]. PCa typically demonstrates early and intense enhancement and brisk “wash-out”. DCE imaging allows quantitative permeability parameters, including K^{trans} (influx volume transfer coefficient), k_{ep} (efflux volume transfer coefficient), and $iAUC$ (area under the gadolinium concentration curve) to be calculated. AUC of DCE-MRI for PCa detection ranges between 0.82 and 0.86, and addition of DCE-MRI to T2WI significantly improves PCa detection compared with T2WI alone [15].

PI-RADS and other assessment systems

Like any rapidly developing technology, prostate mpMRI has been subject to certain impediments, including marked variability in performance, interpretation, and reporting of examinations. The many factors that contribute to the “multiparametric” nature of MRI, and refinements over time, make standardization a highly complex task. Recognizing this, an international working group was assembled in 2007 to develop a research strategy to overcome some of these limitations. As a result of this collaboration, the European Society of Urogenital Radiology published the *Prostate Imaging-Reporting and Data System* (PI-RADS) in 2012 [16]. The primary goals of PI-RADS were to: establish minimum technical parameters for mpMRI performance, standardize reporting terminology, and improve communication of risk assessment between radiologists and urologists.

PI-RADS was modeled after similar efforts that took place in mammography in the 1990s leading to the creation of Breast Imaging Reporting and Data System that led to a revolution in breast cancer management [17]. PI-RADS version 1 was based on a combination of literature evidence and expert opinion and has been validated in several research and clinical settings. A recent meta-analysis evaluated 14 studies (1,785 patients) that used PI-RADS criteria for PCa localization. Pooled sensitivity and specificity were 78% and 79%,

respectively [18]. Fig. 1 demonstrates examples of peripheral zone lesions of varying suspicion on T2WI and the likelihood of clinically significant PCa detection.

A joint steering committee formed by the American College of Radiology, the European Society of Urogenital Radiology, and the AdMeTech Foundation recently proposed an updated version of recommendations, PI-RADS version 2 (v2), released in 2014 [19]. There are a few important differences between PI-RADS v2 and PI-RADS v1. The concept of a “dominant sequence” has been introduced, acknowledging that DWI is the most important sequence for assessment of the peripheral zone and T2WI is the most important sequence for assessment of the transition zone. There is decreased reliance on DCE imaging. The routine use of magnetic resonance spectroscopy is no longer recommended. Finally, the overall assessment is now reported using a 5-point scale for each lesion; suspicion of PCa was previously conveyed via a 1 to 15 scale in PI-RADS v1. PI-RADS v2 has yet to be widely validated, but preliminary studies are promising. Vargas et al. recently evaluated the diagnostic accuracy of PI-RADS v2 in 150 men with 169 tumors, using whole-mount histopathology as the reference standard. PI-RADS v2 correctly identified 94% to 95% of PCa foci >0.5 ml [20].

Although endorsed by a number of societies, PI-RADS v2 is not the only validated prostate MRI scoring system in use. A scoring system, similar to PI-RADS v2, but more quantitative, was developed early on at University of California, Los Angeles (UCLA) [21–24]. PI-RADS recommends a qualitative evaluation of DWI to accommodate the variation in techniques. As employed in the UCLA scoring system, a quantitative evaluation using the ADC can be undertaken if all parameters, including image platform, are kept constant. Apart from being more quantitative, the UCLA scoring system lends slightly more weight to DWI and slightly devalues transition zone lesions.

The National Institutes of Health (NIH) prostate imaging group has also developed a prostate MRI scoring system [4,25,26]. The NIH system uses a 3-point Likert scale to assign a suspicion of low, moderate, or high based on the number of pulse sequences on which an abnormality is identified. Muller et al. recently published results of an interreader study evaluating PI-RADS v2 and the in-house scoring system used at the NIH. Moderate interreader agreement for PI-RADS v2 was found, but MRI scoring was more uniform between readers using the 3-point system [27].

The MRI score is the single most important determinant of PCa risk. In a recent prospective study of 1,042 men who underwent mpMRI followed by magnetic resonance or ultrasound fusion biopsy, lesion suspicion score was the most powerful predictor of clinically significant cancer detection (odd ratio = 6.5, $P < 0.01$) [28]. Each scoring system provides progressive detection of PCa and clinically significant disease (CSD) as suspicion score increases. A comparison of the 3 referenced scoring systems is shown in Fig. 2 [3,29,30] and Table 1. Scoring systems will likely evolve as longer term outcome data become available, which should decrease the reliance on correlation with pathologic findings, which may be limited by pathologist interobserver variability [31]. The true value of prostate mpMRI will lie in its ability to predict patient outcomes.

MRI prediction of PCa aggressiveness

A measure of how accurately men in AS are staged is a reduction in the likelihood of reclassification on subsequent biopsy. Emerging evidence suggests that mpMRI has the necessary sensitivity and specificity to select appropriate candidates. In a retrospective study, Turkbey et al. [4], showed that mpMRI outperformed conventional clinical criteria (D'Amico, Epstein, and Cancer of the Prostate Risk Assessment) for prediction of AS candidates. A recent systematic review by Schoots et al. [32] concluded that mpMRI is useful for the detection of clinically significant PCa at initial assessment among men considering AS. Pooled data showed that identification of a lesion on mpMRI increased the likelihood of Gleason upgrading on radical prostatectomy (43% vs. 27%).

Our group has previously published results on the likelihood of reclassification among men being considered for AS, undergoing confirmatory magnetic resonance-ultrasound fusion biopsy [21]. When stratified by mpMRI suspicion score, the likelihood of reclassification was 24% to 29% for grade 0 to 3 targets, 45% for grade 4 targets and 100% for grade 5 targets. Similar results have also been reported by our group and other groups regarding the use of serial MRI among patients on AS [33–35]. Presently, we are reluctant to enroll a man in the AS program until mpMRI and guided biopsy have been obtained. In addition to the overall mpMRI assessment category, several authors have evaluated the contribution of individual mpMRI sequences to PCa risk stratification [36–38]. Both DWI and DCE are promising tools for this type of evaluation, because they provide quantitative assessment of tumor features.

Turkbey et al. [39] evaluated the correlation between tumor ADC and clinical risk scores in PCa and demonstrated an inverse relationship between tumor ADC and Gleason and D'Amico risk scores, concluding that ADC may be useful in predicting PCa aggressiveness. These results have subsequently been confirmed by others [40–42]. Chamie et al. recently evaluated the use of ADC for delineating CSD in a radical prostatectomy cohort. Sensitivity and NPV for CSD using Epstein criteria alone were 0.79 and 0.68, respectively. These improved to 0.93 and 0.84, respectively, with the addition of tumor ADC [3]. Taken together, these findings suggest that ADC has the potential to be used as an important noninvasive imaging biomarker for PCa risk assessment.

To date, there has been less investigation into quantitative DCE imaging parameters for PCa risk assessment, but preliminary work suggests these too may have use in this regard. Chung et al. [43] recently evaluated whether k^{trans} , k_{ep} , and $iAUC$ correlated with National Comprehensive Cancer Network Risk Group and Gleason score in a cohort of 58 patients being evaluated during the course of radiation treatment. The authors reported that $iAUC$ was significantly different for peripheral zone tumors when stratified by low or intermediate, or high risk National Comprehensive Cancer Network categories and Gleason score. Cho et al. [44] also recently evaluated optimal cut-off values of DCE-MRI perfusion parameters for defining PCa aggressiveness and found k^{trans} and k_{ep} were significantly correlated with Gleason Score. Larger studies will be necessary to validate these findings.

PCa clinical risk stratification

Clinical risk stratification is traditionally done with a combination of DRE, PSA, and biopsy Gleason Score. These 3 features are combined into a clinical nomogram (Partin table) to predict the likelihood of organ-confined disease [45]. Clinical risk stratification is suboptimal. Overall, 25% to 30% of patients with extracapsular extension (ECE) are understaged preoperatively [46]. Compared to organ-confined disease, PCa with ECE has a worse overall and cancer-specific survival [47,48]. Preoperative identification of ECE or SVI can influence therapy selection and the decision to spare the neurovascular bundles during surgery [49], as shown in Fig. 3.

Over the last decade there has been renewed interest in mpMRI for preoperative PCa staging. Improved spatial resolution now allows direct visualization of the prostate capsule. Feng et al. [50] recently evaluated whether mpMRI improved clinical accuracy of the Partin and Memorial Sloan Kettering nomograms for estimating ECE risk. AUC of the Partin and MSK nomograms were 0.85 and 0.86, respectively. With the addition of preoperative mpMRI, AUCs improved to 0.92 and 0.94, respectively. In a retrospective study of 131 patients who underwent preoperative mpMRI followed by radical prostatectomy, Soyulu et al. reported specificity of 96.6% to 98.3% and PPV of 70% to 79% for prediction of SVI based on combined review of T2WI and DWI [51]. Multiple additional similar studies have demonstrated the benefit of mpMRI for preoperative prediction of ECE and SVI [52–55]. The question of whether an ERC is necessary for surgical staging of PCa remains unanswered. Staging accuracy was initially reported to be superior with use of an ERC [56,57], but a recent meta-analysis showed no difference in sensitivity for the detection of EPE with use of an ERC compared with a body phased-array surface coil, though there was a slight increase in sensitivity for detection of SVI [58]. Use of an ERC probably improves overall staging accuracy marginally, but adequate staging can be performed with 3.0 T mpMRI and a body surface coil.

Conventional MRI fails to detect up to 60% of metastatic PCa lymph nodes, because most of them are small (<8 mm in diameter) [59]. This problem of detection is compounded, because as many as 41% of metastatic PCa lymph nodes are located outside the routine pelvic lymph node dissection template [60]. A potential solution is the use of DWI. A recent prospective study in which more than 4,000 lymph nodes were resected from 120 patients with PCa or bladder cancer demonstrated diagnostic accuracy of 90% to 92% for metastatic lymph nodes, of which more than 75% were less than 3 mm in short-axis diameter [61]. Other investigators have recently reported less promising results for DWI. In a prospective study of patients undergoing superextended lymph node dissection, Van den Bergh et al. [62] reported per patient sensitivity of 36.1% for DWI.

An alternative solution is the use of ultrasmall superparamagnetic particles of iron oxide (USPIO)-enhanced MRI. USPIOs are taken up by macrophages within healthy lymph nodes; the iron oxide crystalline core produces susceptibility and reduces T2WI-signal intensity. The decreased signal intensity denotes a healthy lymph node. Malignant lymph nodes, by contrast, contain very few macrophages and do not take up USPIO. Lack of USPIO uptake creates positive contrast and malignant nodes appear bright. Birkhauser et al. reported results of the combined use of DWI and USPIO MRI for the detection of normal-sized metastatic

nodes in patients with bladder cancer and PCa. Per patient sensitivity and specificity ranged from 65% to 75% and 93% to 96%, respectively [63].

Limitations

The most important limitation of mpMRI is the failure to detect significant PCa in a yet-to-be-defined number of cases. The NPV of mpMRI for exclusion of significant PCa varies depending on the study and the manner in which significant PCa is established. Itatani et al. recently reported the *clinical* NPV of mpMRI in a cohort of 193 men suspected of harboring PCa with an initial negative mpMRI. They reported a NPV of 89.6% for mpMRI; absence of PCa was defined by stable PSA, negative DRE and conventional systematic biopsy [64]. Using whole-mount histopathology as the reference standard, Le et al. [65] reported that mpMRI failed to identify 28% of Gleason >7 PCa foci and 28% of tumors >1 cm. There are many proposed explanations for failure of mpMRI to detect PCa—the tumor may not exhibit a solid growth pattern or incite a large desmoplastic reaction, or it may be obscured by surrounding benign changes, such as benign prostatic hyperplasia, hemorrhage, or prostatitis. MRI-invisible PCa has also been shown to be histologically distinct from those detected [66]. Owing to this important limitation, we do not believe a negative mpMRI is currently sufficient to obviate the need for at least 1 systematic prostate biopsy among men in whom biopsy would otherwise be indicated.

Another important limitation of mpMRI is the tendency to underestimate tumor volume, compared with histopathology. Le Nobin et al. [67] recently reported that mpMRI-estimated tumor volume was 18.5% smaller than actual histologic tumor volume. The magnitude of tumor volume underestimation was directly related to MRI suspicion score and Gleason Score. The tendency of mpMRI to underestimate true pathologic tumor volume has also been reported by several other authors [68,69]. Underestimation of tumor volume on mpMRI, especially in cases of clinically significant disease, may not only affect conventional treatment decisions but also affects the use of novel focal therapeutics.

Another mpMRI limitation is that the diagnostic accuracy is heavily dependent upon reader experience [70]. Tay et al. recently explored the effect of reader experience in a retrospective study of 120 men evaluated with preoperative mpMRI done for staging. Sensitivity and specificity for detection of ECE for the general reader were 77% and 44%, respectively. These improved to 86% and 81% with a more experienced reader [71]. As prostate mpMRI is increasingly used in low-volume settings, standardization of reader experience, and reader training to achieve equivalent outcomes will become an important issue.

Lastly, the cost of widespread use of prostate mpMRI is significant, which is another important potential limitation. As this technology becomes more widely disseminated, appropriate patient selection for mpMRI will become increasingly important. The reader is referred to a separate article in this issue, addressing the economic effect of using MRI and MRI-fusion biopsy for PCa diagnosis.

Future directions

There are many active areas of investigation in prostate mpMRI; most of them are focused on improving PCa detection and characterization. Interpreting prostate mpMRI is a complex

and time-consuming process, so there is considerable interest in using computer-aided diagnosis (CAD) to increase efficiency and accuracy. CAD systems work by extracting information from the mpMRI, often features that are not perceptible to the human eye, such as texture features, and thereby assist the radiologist in interpretation. Kwak et al. [72] recently evaluated a CAD system, using a texture feature-based algorithm with T2WI and DWI, in 244 patients. They reported an AUC of 0.83 for distinguishing PCa from mpMRI-positive benign lesions. Multiple other studies have investigated the use of texture feature analysis in prostate mpMRI with encouraging results [73,74]. These developments are expected to be particularly helpful to readers with less experience.

Restriction spectrum imaging is another promising area of investigation. It is a novel advanced diffusion-based technique that offers several theoretical advantages over conventional DWI, including: reduced spatial distortion, enhanced tumor contrast, and a normalized measure of in vivo cellularity that is potentially more reproducible than ADC. We recently applied this technique to prostate mpMRI and showed that the restriction spectrum imaging-derived cellularity index was associated with aggressive PCa [75].

There is considerable interest in the use of abbreviated prostate mpMRI protocols, such as biparametric MRI, using T2WI and DWI alone. Such protocols have potential for significant time and cost savings. Preliminary studies suggest that biparametric prostate MRI is more accurate for PCa detection than conventional clinical tools, such as PSA and DRE [76] and thus may be a useful screening tool in appropriately selected men. Biparametric protocols can be carried out even faster without the use of an ERC [77].

Lastly, by providing information on tumor location and tumor volume, mpMRI has the potential to guide less radical approaches to PCa, such as focal therapy. Further characterization of prostate tumors through assessment of perfusion, cellular density and vascularity promises to refine these techniques even further.

Conclusion

Prostate mpMRI has become an integral component of PCa management in many urology practices. In terms of risk stratification, evidence supports the use of prostate mpMRI (often followed by targeted biopsy) before enrollment in AS; and for staging of intermediate to high-risk disease, including the decision of whether or not to spare the neurovascular bundles. Despite many advantages, important limitations are failure to detect clinically significant cancer in a yet-to-be-determined number of patients and underestimation of true tumor volume.

Acknowledgments

The project described was supported by Award number R01CA158627 from the National Cancer Institute, United States. The content is solely the responsibility of the authors and does not necessarily represent the official views of the National Cancer Institute or the National Institutes of Health. Additional support was provided by University of California, Los Angeles, United State Clinical and Translational Sciences Institute Grant no. UL1TR000124, the Beckman Coulter Foundation, the Jean Perkins Foundation, and the Steven C. Gordon Family Foundation.

References

1. Fütterer JJ, Briganti A, De Visschere P, et al. Can clinically significant prostate cancer be detected with multiparametric magnetic resonance imaging? A systematic review of the literature. *Eur Urol*. 2015; 68:1045–53. [PubMed: 25656808]
2. Shukla-Dave A, Hricak H, Akin O, et al. Preoperative nomograms incorporating magnetic resonance imaging and spectroscopy for prediction of insignificant prostate cancer. *BJU Int*. 2012; 109:1315–22. [PubMed: 21933336]
3. Chamie K, Sonn GA, Finley DS, et al. The role of magnetic resonance imaging in delineating clinically significant prostate cancer. *Urology*. 2014; 83:369–75. [PubMed: 24468511]
4. Turkbey B, Mani H, Aras O, et al. Prostate cancer: can multiparametric MR imaging help identify patients who are candidates for active surveillance? *Radiology*. 2013; 268:144–52. [PubMed: 23468576]
5. Hricak H, Williams RD, Spring DB, et al. Anatomy and pathology of the male pelvis by magnetic resonance imaging. *Am J Roentgenol*. 1983; 141:1101–10. [PubMed: 6196961]
6. Akin O, Sala E, Moskowitz CS, et al. Transition zone prostate cancers: features, detection, localization, and staging at endorectal MR imaging. *Radiology*. 2006; 239:784–92. [PubMed: 16569788]
7. Li H, Sugimura K, Kaji Y, et al. Conventional MRI capabilities in the diagnosis of prostate cancer in the transition zone. *Am J Roentgenol*. 2006; 186:729–42. [PubMed: 16498100]
8. Qayyum A. Diffusion-weighted imaging in the abdomen and pelvis: concepts and applications. *Radiographics*. 2009; 29:1797–810. [PubMed: 19959522]
9. Lövlblad KO, Laubach HJ, Baird AE, et al. Clinical experience with diffusion-weighted MR in patients with acute stroke. *Am J Neuroradiol*. 1998; 19:1061–6. [PubMed: 9672012]
10. Jie C, Rongbo L, Ping T. The value of diffusion-weighted imaging in the detection of prostate cancer: a meta-analysis. *Eur Radiol*. 2014; 24:1929–41. [PubMed: 24865693]
11. Henderson DR, de Souza NM, Thomas K, et al. Nine-year follow-up for a study of diffusion-weighted magnetic resonance imaging in a prospective prostate cancer active surveillance cohort. *Eur Urol*. 2015
12. Erbersdobler A, Isbarn H, Dix K, et al. Prognostic value of microvessel density in prostate cancer: a tissue microarray study. *World J Urol*. 2010; 28:687–92. [PubMed: 19714336]
13. Mucci LA, Powolny A, Giovannucci E, et al. Prospective study of prostate tumor angiogenesis and cancer-specific mortality in the health professionals follow-up study. *J Clin Oncol*. 2009; 27:5627–33. [PubMed: 19858401]
14. Brawer MK, Deering RE, Brown M, Preston SD, Bigler SA. Predictors of pathologic stage in prostatic carcinoma. The role of neovascularity. *Cancer*. 1994; 73:678–87. [PubMed: 7507798]
15. Tan CH, Hobbs BP, Wei W, Kundra V. Dynamic contrast-enhanced MRI for the detection of prostate cancer: meta-analysis. *Am J Roentgenol*. 2015; 204:W439–48. [PubMed: 25794093]
16. Barentsz JO, Richenberg J, Clements R, et al. ESUR prostate MR guidelines 2012. *Eur Radiol*. 2012; 22:746–57. [PubMed: 22322308]
17. D’Orsi C, Sickles E, Mendelson E, Morris E. ACR BI-RADS[®] Atlas, Breast Imaging Reporting and Data System Reston, VA: American College of Radiology; 2013
18. Hamoen EH, de Rooij M, Witjes JA, Barentsz JO, Rovers MM. Use of the prostate imaging reporting and data system (PI-RADS) for prostate cancer detection with multiparametric magnetic resonance imaging: a diagnostic meta-analysis. *Eur Urol*. 2015; 67:1112–21. [PubMed: 25466942]
19. Weinreb JC, Barentsz JO, Choyke PL, et al. PI-RADS prostate imaging—reporting and data system: 2015, version 2. *Eur Urol*. 2015:16–40. [PubMed: 26427566]
20. Vargas HA, Hötter AM, Goldman DA, et al. Updated prostate imaging reporting and data system (PI-RADS v2) recommendations for the detection of clinically significant prostate cancer using multiparametric MRI: critical evaluation using whole-mount pathology as standard of reference. *Eur Radiol*. 2015
21. Hu JC, Chang E, Natarajan S, et al. Targeted prostate biopsy in select men for active surveillance: do the Epstein criteria still apply? *J Urol*. 2014; 192:385–90. [PubMed: 24512956]

22. Sonn GA, Natarajan S, Margolis DJ, et al. Targeted biopsy in the detection of prostate cancer using an office based magnetic resonance ultrasound fusion device. *J Urol*. 2013; 189:86–91. [PubMed: 23158413]
23. Le JD, Stephenson S, Brugger M, et al. Magnetic resonance imaging-ultrasound fusion biopsy for prediction of final prostate pathology. *J Urol*. 2014; 192:1367–73. [PubMed: 24793118]
24. Sonn GA, Chang E, Natarajan S, et al. Value of targeted prostate biopsy using magnetic resonance-ultrasound fusion in men with prior negative biopsy and elevated prostate-specific antigen. *Eur Urol*. 2014; 65:809–15. [PubMed: 23523537]
25. Rais-Bahrami S, Siddiqui MM, Turkbey B, et al. Utility of multiparametric magnetic resonance imaging suspicion levels for detecting prostate cancer. *J Urol*. 2013; 190:1721–7. [PubMed: 23727310]
26. Rastinehad AR, Turkbey B, Salami SS, et al. Improving detection of clinically significant prostate cancer: magnetic resonance imaging/transrectal ultrasound fusion guided prostate biopsy. *J Urol*. 2014; 191:1749–54. [PubMed: 24333515]
27. Muller BG, Shih JH, Sankineni S, et al. Prostate cancer: interobserver agreement and accuracy with the revised prostate imaging reporting and data system at multiparametric MR imaging. *Radiology*. 2015 142818.
28. Filson CP, Natarajan S, Margolis DJ, et al. Prostate cancer detection with magnetic resonance-ultrasound fusion biopsy: the role of systematic and targeted biopsies. *Cancer*. 2016
29. Cash H, Maxeiner A, Stephan C, et al. The detection of significant prostate cancer is correlated with the prostate imaging reporting and data system (PI-RADS) in MRI/transrectal ultrasound fusion biopsy. *World J Urol*. 2015
30. Pinto PA, Chung PH, Rastinehad AR, et al. Magnetic resonance imaging/ultrasound fusion guided prostate biopsy improves cancer detection following transrectal ultrasound biopsy and correlates with multiparametric magnetic resonance imaging. *J Urol*. 2011; 186:1281–5. [PubMed: 21849184]
31. Evans AJ, Henry PC, Van der Kwast TH, et al. Interobserver variability between expert urologic pathologists for extraprostatic extension and surgical margin status in radical prostatectomy specimens. *Am J Surg Pathol*. 2008; 32:1503–12. [PubMed: 18708939]
32. Schoots IG, Petrides N, Giganti F, et al. Magnetic resonance imaging in active surveillance of prostate cancer: a systematic review. *Eur Urol*. 2015; 67:627–36. [PubMed: 25511988]
33. Da Rosa MR, Milot L, Sugar L, et al. A prospective comparison of MRI-US fused targeted biopsy versus systematic ultrasound-guided biopsy for detecting clinically significant prostate cancer in patients on active surveillance. *J Magn Reson Imaging*. 2015; 41:220–5. [PubMed: 25044935]
34. Walton Diaz A, Shakir NA, George AK, et al. Use of serial multiparametric magnetic resonance imaging in the management of patients with prostate cancer on active surveillance. *Urol Oncol*. 2015; 33:202.e1–7.
35. Felker ER, Wu J, Natarajan S, et al. Serial MRI in active surveillance of prostate cancer: incremental value. *J Urol*. 2015
36. Rosenkrantz AB, Ream JM, Nolan P, Rusinek H, Deng FM, Taneja SS. Prostate Cancer: utility of whole-lesion apparent diffusion coefficient metrics for prediction of biochemical recurrence after radical prostatectomy. *Am J Roentgenol*. 2015; 205:1208–14. [PubMed: 26587927]
37. Cheikh AB, Girouin N, Colombel M, et al. Evaluation of T2-weighted and dynamic contrast-enhanced MRI in localizing prostate cancer before repeat biopsy. *Eur Radiol*. 2009; 19:770–8. [PubMed: 18925403]
38. Jung SI, Donati OF, Vargas HA, Goldman D, Hricak H, Akin O. Transition zone prostate cancer: incremental value of diffusion-weighted endorectal MR imaging in tumor detection and assessment of aggressiveness. *Radiology*. 2013; 269:493–503. [PubMed: 23878284]
39. Turkbey B, Shah VP, Pang Y, et al. Is apparent diffusion coefficient associated with clinical risk scores for prostate cancers that are visible on 3-T MR images? *Radiology*. 2011; 258:488–95. [PubMed: 21177390]
40. De Cobelli F, Ravelli S, Esposito A, et al. Apparent diffusion coefficient value and ratio as noninvasive potential biomarkers to predict prostate cancer grading: comparison with prostate

- biopsy and radical prostatectomy specimen. *Am J Roentgenol.* 2015; 204:550–7. [PubMed: 25714284]
41. Nowak J, Malzahn U, Baur AD, et al. The value of ADC, T2 signal intensity, and a combination of both parameters to assess Gleason score and primary Gleason grades in patients with known prostate cancer. *Acta Radiol.* 2014
 42. Boesen L, Chabanova E, Løgager V, Balslev I, Thomsen HS. Apparent diffusion coefficient ratio correlates significantly with prostate cancer gleason score at final pathology. *J Magn Reson Imaging.* 2015; 42:446–53. [PubMed: 25408104]
 43. Chung MP, Margolis D, Mesko S, Wang J, Kupelian P, Kamrava M. Correlation of quantitative diffusion-weighted and dynamic contrast-enhanced MRI parameters with prognostic factors in prostate cancer. *J Med Imaging Radiat Oncol.* 2014; 58:588–94. [PubMed: 25196228]
 44. Cho E, Chung DJ, Yeo DM, et al. Optimal cut-off value of perfusion parameters for diagnosing prostate cancer and for assessing aggressiveness associated with Gleason score. *Clin Imaging.* 2015; 39:834–40. [PubMed: 26001659]
 45. Eifler JB, Feng Z, Lin BM, et al. An updated prostate cancer staging nomogram (Partin tables) based on cases from 2006 to 2011. *BJU Int.* 2013; 111:22–9. [PubMed: 22834909]
 46. Cooperberg MR, Lubeck DP, Mehta SS, Carroll PR. CaPSURE. Time trends in clinical risk stratification for prostate cancer: implications for outcomes (data from CaPSURE). *J Urol.* 2003; 170:S21–5. discussion S6–S27. [PubMed: 14610406]
 47. Mikel Hubanks J, Boorjian SA, Frank I, et al. The presence of extracapsular extension is associated with an increased risk of death from prostate cancer after radical prostatectomy for patients with seminal vesicle invasion and negative lymph nodes. *Urol Oncol.* 2014; 32:26.e1–e7.
 48. Tollefson MK, Karnes RJ, Rangel LJ, Bergstralh EJ, Boorjian SA. The impact of clinical stage on prostate cancer survival following radical prostatectomy. *J Urol.* 2013; 189:1707–12. [PubMed: 23159265]
 49. McClure TD, Margolis DJ, Reiter RE, et al. Use of MR imaging to determine preservation of the neurovascular bundles at robotic-assisted laparoscopic prostatectomy. *Radiology.* 2012; 262:874–83. [PubMed: 22274837]
 50. Feng TS, Sharif-Afshar AR, Wu J, et al. Multiparametric MRI improves accuracy of clinical nomograms for predicting extracapsular extension of prostate cancer. *Urology.* 2015; 86:332–7. [PubMed: 26194289]
 51. Soylu FN, Peng Y, Jiang Y, et al. Seminal vesicle invasion in prostate cancer: evaluation by using multiparametric endorectal MR imaging. *Radiology.* 2013; 267:797–806. [PubMed: 23440325]
 52. Baco E, Rud E, Vlatkovic L, et al. Predictive value of magnetic resonance imaging determined tumor contact length for extracapsular extension of prostate cancer. *J Urol.* 2015; 193:466–72. [PubMed: 25150643]
 53. Wang L, Hricak H, Kattan MW, Chen HN, Scardino PT, Kuroiwa K. Prediction of organ-confined prostate cancer: incremental value of MR imaging and MR spectroscopic imaging to staging nomograms. *Radiology.* 2006; 238:597–603. [PubMed: 16344335]
 54. Gupta RT, Faridi KF, Singh AA, et al. Comparing 3-T multiparametric MRI and the Partin tables to predict organ-confined prostate cancer after radical prostatectomy. *Urol Oncol.* 2014; 32:1292–9. [PubMed: 24863013]
 55. Finley DS, Margolis D, Raman SS, et al. Fine-tuning robot-assisted radical prostatectomy planning with MRI. *Urol Oncol.* 2013; 31:766–75. [PubMed: 21906964]
 56. Heijmink SW, Fütterer JJ, Hambroek T, et al. Prostate cancer: body-array versus endorectal coil MR imaging at 3 T—comparison of image quality, localization, and staging performance. *Radiology.* 2007; 244:184–95. [PubMed: 17495178]
 57. Fütterer JJ, Engelbrecht MR, Jager GJ, et al. Prostate cancer: comparison of local staging accuracy of pelvic phased-array coil alone versus integrated endorectal-pelvic phased-array coils. Local staging accuracy of prostate cancer using endorectal coil MR imaging. *Eur Radiol.* 2007; 17:1055–65. [PubMed: 17024497]
 58. de Rooij M, Hamoen EH, Witjes JA, Barentsz JO, Rovers MM. Accuracy of magnetic resonance imaging for local staging of prostate cancer: a diagnostic meta-analysis. *Eur Urol.* 2015

59. Hövels AM, Heesakkers RA, Adang EM, et al. The diagnostic accuracy of CT and MRI in the staging of pelvic lymph nodes in patients with prostate cancer: a meta-analysis. *Clin Radiol*. 2008; 63:387–95. [PubMed: 18325358]
60. Heesakkers RA, Jager GJ, Hövels AM, et al. Prostate cancer: detection of lymph node metastases outside the routine surgical area with ferumoxtran-10-enhanced MR imaging. *Radiology*. 2009; 251:408–14. [PubMed: 19401573]
61. Thoeny HC, Froehlich JM, Triantafyllou M, et al. Metastases in normal-sized pelvic lymph nodes: detection with diffusion-weighted MR imaging. *Radiology*. 2014; 273:125–35. [PubMed: 24893049]
62. Van den Bergh L, Lerut E, Haustermans K, et al. Final analysis of a prospective trial on functional imaging for nodal staging in patients with prostate cancer at high risk for lymph node involvement. *Urol Oncol*. 2015; 33:109.e23–e31.
63. Birkhäuser FD, Studer UE, Froehlich JM, et al. Combined ultrasmall superparamagnetic particles of iron oxide-enhanced and diffusion-weighted magnetic resonance imaging facilitates detection of metastases in normal-sized pelvic lymph nodes of patients with bladder and prostate cancer. *Eur Urol*. 2013; 64:953–60. [PubMed: 23916692]
64. Itatani R, Namimoto T, Atsugi S, et al. Negative predictive value of multiparametric MRI for prostate cancer detection: outcome of 5-year follow-up in men with negative findings on initial MRI studies. *Eur J Radiol*. 2014; 83:1740–5. [PubMed: 25048979]
65. Le JD, Tan N, Shkolyar E, et al. Multifocality and prostate cancer detection by multiparametric magnetic resonance imaging: correlation with whole-mount histopathology. *Eur Urol*. 2015; 67:569–76. [PubMed: 25257029]
66. Rosenkrantz AB, Mendrinos S, Babb JS, Taneja SS. Prostate cancer foci detected on multiparametric magnetic resonance imaging are histologically distinct from those not detected. *J Urol*. 2012; 187:2032–8. [PubMed: 22498205]
67. Le Nobin J, Rosenkrantz AB, Villers A, et al. Image guided focal therapy for magnetic resonance imaging visible prostate cancer: defining a 3-dimensional treatment margin based on magnetic resonance imaging histology co-registration analysis. *J Urol*. 2015; 194:364–70. [PubMed: 25711199]
68. Nakashima J, Tanimoto A, Imai Y, et al. Endorectal MRI for prediction of tumor site, tumor size, and local extension of prostate cancer. *Urology*. 2004; 64:101–5. [PubMed: 15245944]
69. Ponchiotti R, Di Loro F, Fanfani A, Amorosi A. Estimation of prostate cancer volume by endorectal coil magnetic resonance imaging vs. pathologic volume. *Eur Urol*. 1999; 35:32–5.
70. Ruprecht O, Weisser P, Bodelle B, Ackermann H, Vogl TJ. MRI of the prostate: interobserver agreement compared with histopathologic outcome after radical prostatectomy. *Eur J Radiol*. 2012; 81:456–60. [PubMed: 21354732]
71. Tay KJ, Gupta RT, Brown AF, Silverman RK, Polascik TJ. Defining the incremental utility of prostate multiparametric magnetic resonance imaging at standard and specialized read in predicting extracapsular extension of prostate cancer. *Eur Urol*. 2015
72. Kwak JT, Xu S, Wood BJ, et al. Automated prostate cancer detection using T2-weighted and high-b-value diffusion-weighted magnetic resonance imaging. *Med Phys*. 2015; 42:2368–78. [PubMed: 25979032]
73. Wibmer A, Hricak H, Gondo T, et al. Haralick texture analysis of prostate MRI: utility for differentiating non-cancerous prostate from prostate cancer and differentiating prostate cancers with different Gleason scores. *Eur Radiol*. 2015; 25:2840–50. [PubMed: 25991476]
74. Vignati A, Mazzetti S, Giannini V, et al. Texture features on T2-weighted magnetic resonance imaging: new potential biomarkers for prostate cancer aggressiveness. *Phys Med Biol*. 2015; 60:2685–701. [PubMed: 25768265]
75. Liss MA, White NS, Parsons JK, et al. MRI-derived restriction spectrum imaging cellularity index is associated with high grade prostate cancer on radical prostatectomy specimens. *Front Oncol*. 2015; 5:30. [PubMed: 25741473]
76. Rais-Bahrami S, Siddiqui MM, Vourganti S, et al. Diagnostic value of biparametric magnetic resonance imaging (MRI) as an adjunct to prostate-specific antigen (PSA)-based detection of prostate cancer in men without prior biopsies. *BJU Int*. 2015; 115:381–8. [PubMed: 24447678]

77. Turkbey B, Merino MJ, Gallardo EC, et al. Comparison of endorectal coil and nonendorectal coil T2W and diffusion-weighted MRI at 3 Tesla for localizing prostate cancer: correlation with whole-mount histopathology. *J Magn Reson Imaging*. 2014; 39:1443–8. [PubMed: 24243824]

Author Manuscript

Author Manuscript

Author Manuscript

Author Manuscript

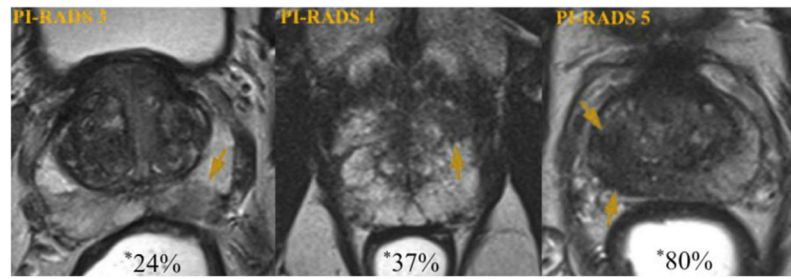


Fig. 1. Likelihood of significant prostate cancer detection by MRI suspicion. Axial T2-weighted prostate images demonstrating peripheral zone lesions (arrows) of increasing suspicion. Examples are of a PI-RADS 3 target (left), a PI-RADS 4 target (center), and a PI-RADS 5 target (right). Percentages shown with asterisk represent likelihood of targeted biopsy revealing a cancer of Gleason Score 7 or greater, based on UCLA data ($n = 1,200$) (78). *Modified and reprinted with permission from *European Urology* 69(1); Weinreb et al. [19]. Copyright 2016, with permission from Elsevier. (Color version of figure is available online.)

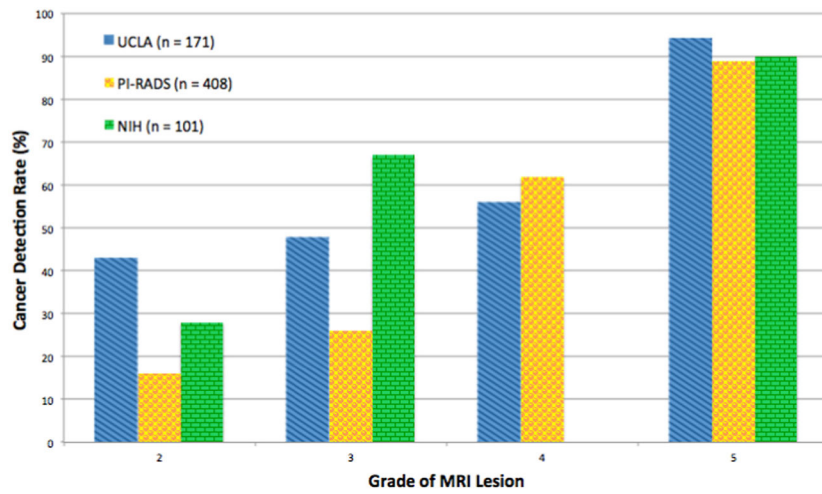


Fig. 2. Prostate cancer detection rates for 3 different scoring systems, stratified by level of suspicion on MRI. A progressive increase in prostate cancer detection with increasing suspicion score is consistently shown for each of the 3 systems. (Data shown are for detection of all PCa, but a qualitatively similar pattern is also apparent for clinically significant disease). (Color version of figure is available online.)

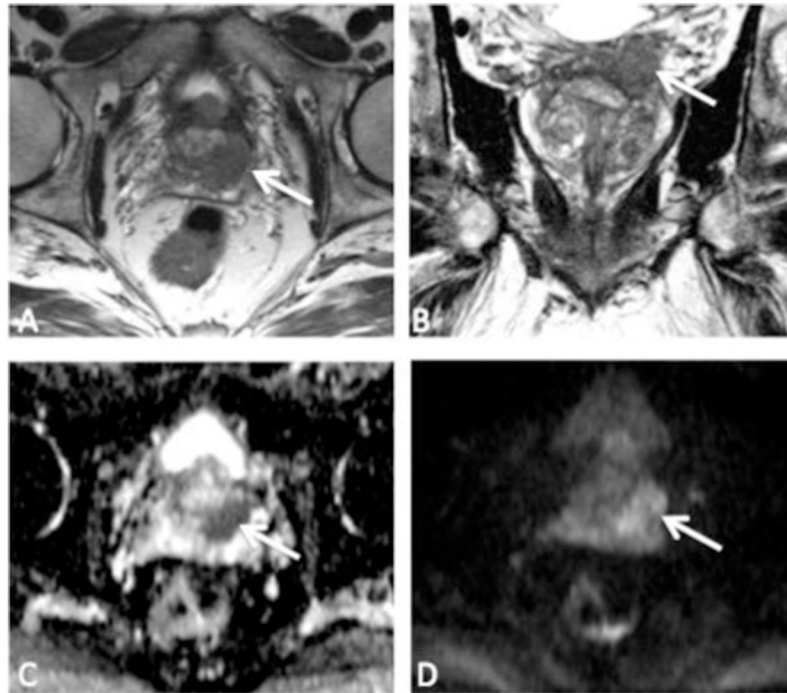


Fig. 3.

A 64-year-old man referred for possible enrollment into active surveillance, after conventional biopsy revealed Gleason 3 + 3 in 10% of 1 core. Top row—T2-weighted images, (A) (axial) and (B) (coronal). There is a large tumor in the left peripheral zone base (arrows), with findings suggestive of extracapsular extension (ECE) and involvement of the left seminal vesicle (SV). Bottom row—diffusion-weighted images, (C) (apparent diffusion coefficient map) and (D) (high *b*-value). There is markedly restricted diffusion within the tumor. Final pathology demonstrated Gleason 4 + 4 at the left base with ECE and SV invasion.

Table 1

Comparison of 3 MRI Scoring Systems

	UCLA	PI-RADS version 2	NIH
Pulse sequences	T2, DWI, DCE	T2, DWI, DCE	T2, DWI, DCE
Dominant sequence	DWI for PZ and TZ	DWI for PZ; T2 for TZ	No
DWI assessment	Quantitative (ADC)	Qualitative	Qualitative
DCE assessment	Semiquantitative	Qualitative	Qualitative
Scale	1–5	1–5	Low/intermediate/high
Externally validated	No	Yes	No

Comparison of the 3 prostate mpMRI scoring systems discussed in the text.

PZ = peripheral zone; TZ = transition zone.